PROCEEDINGS OF SCIENCE

Unveiling the Origin of the Fermi/eRosita Bubbles

Hsiang-Yi Karen Yang[a,b,c,*]

[a] *Institute of Astronomy, National Tsing Hua University, No. 101, Sec. 2, Kuang-Fu Rd., Hsinchu, Taiwan (R.O.C.)*
[b] *Department of Physics, National Tsing Hua University, No. 101, Sec. 2, Kuang-Fu Rd., Hsinchu, Taiwan (R.O.C.)*
[c] *Physics Division, National Center for Thoretical Sciences, Taipei, Taiwan (R.O.C.)*

E-mail: hyang@phys.nthu.edu.tw

The newly launched eRosita X-ray satellite revealed two gigantic bubbles extending to $\sim 80^\circ$ above and below the Galactic center (GC) in the Milky Way Galaxy. The morphology of these *eRosita* bubbles bears a remarkable resemblance to the *Fermi* bubbles discovered in the gamma-ray band by the Fermi Gamma-ray Space Telescope in 2010, suggesting that they may share the same origin. The symmetry about the GC of the *Fermi/eRosita* bubbles suggests that they likely originate from powerful energy injections from the GC sometime in the past, such as a nuclear starburst, or activity from the central supermassive black hole (SMBH). In this proceedings, I will briefly review the progress made in terms of our understanding of the physical origin of the bubbles. In particular, I will highlight the importance of the new observational constraints brought by the *eRosita* mission, and discuss recent simulation results that support a scenario where the *Fermi/eRosita* bubbles are simultaneously generated by past jet activity of the SMBH a few million years ago.

**** The 27th European Cosmic Ray Symposium, ****
**** 25-29 July 2022*
**** Nijmegen, the Netherlands ****

[*]Speaker

PoS(ECRS)023

1. Introduction

One of the most important discoveries of the *Fermi* Gamma-ray Space Telescope is the *Fermi* bubbles, two giant gamma-ray bubbles extending to $\sim 50-55$ degrees above and below the Galactic center (GC) [1]. The large integrated gamma-ray luminosity ($\sim 10^{37}$ erg s^{-1}) and symmetry about the GC suggest that the bubbles likely originate from energetic outbursts from the GC some time in the past, such as a nuclear starburst or activity of the central active galactic nucleus (AGN). Because of their proximity, there is an ample amount of multi-messenger observational data with unprecedented details that provide crucial constraints on the formation mechanisms of the bubbles. The gamma-ray bubbles have counterpart emission in the microwave band, called "microwave haze" [2, 3]. In X-ray, the edges of the *Fermi* bubbles are also spatially coincident with arc features detected in the early 2000s [4] as well as the North Polar Spur (NPS), the most prominent feature in the northern hemisphere observed by the ROSAT X-ray satellite [5]. Mostly recently, the *eRosita* X-ray mission has further revealed two gigantic *eRosita* bubbles, with even larger sizes than the gamma-ray bubbles [6]. Since the discovery of the *Fermi* bubbles in 2010, dozens of theoretical models have been proposed to explain their origin. However, given the stringent observational constraints, it has been a great challenge for any theoretical model to reproduce all the spatially resolved, multi-messenger observational data.

Over the past decades, there have been numerous efforts in the community, both observationally and theoretically, in order to understand the physical origin of the *Fermi* bubbles and their multi-wavelength counterparts. Since it is impossible to review every related work in detail in this Conference Proceedings, this article would instead aim to report the current status on this subject and summarize some of the important findings, particularly focusing on recent advancements. This Conference Proceedings is based on the highlight talk "Unveiling the Origin of the Fermi/eRosita bubbles" at the 27th Eupopean Cosmic Ray Symposium regarding the recent publication of [7]. We therefore refer the readers to [7] for more details as well as [8] for a detailed review of the observational data and theoretical models up to the year of 2018.

2. Multi-messenger Observations

The vicinity of the *Fermi/eRosita* bubbles has been observed in detail using multi-messenger observations. The gamma-ray bubbles are observed between 1 to $\sim$ 100 GeV and have very hard spectrum (spectral index of -2) compared to other components in the gamma-ray sky. The *Fermi* bubbles alone have many unique features, including the hard spectrum, smooth surface, sharp edges, and nearly flat intensity distribution [1], each of which carries important information about the bubble formation mechanisms. For instance, assuming the gamma-ray emission is generated by inverse-Compton (IC) scattering of the interstellar radiation field (ISRF) by cosmic-ray electrons (CRe) (i.e., the *leptonic* scenario), the hard spectrum puts a very stringent constraint on the formation time of the bubbles to be within a few Myr, which is the synchrotron and IC cooling times of CRe at hundreds of GeV. Their smooth surface indicates that there is no rigorous hydrodynamic instabilities occurring on the scales comparable to the bubble sizes. The sharp edges of the bubbles suggest suppression of CR diffusion at the bubble surface. The nearly flat intensity distribution also provides crucial information about the three-dimensional (3D) spatial distributions of the CRs. In particular, it rules out models with CRs distributed in a thin shell near the bubble surface that would project into a limb-brightened intensity profile, e.g., as predicted in some of the early models based on shock acceleration; models that predict uniform gamma-ray emissivities that would produce centrally-brightened intensity distributions are also disfavored [see references in 8]. The more recent compilation of the *Fermi* data [9] confirmed the initial results, but revealed that there is an exponential cutoff at $\sim$ 110 GeV in the gamma-ray spectrum, and that the gamma-ray spectrum is remarkably latitude independent. Considering the effects of line-of-sight projections, the spatially uniform gamma-ray spectrum provides extremely tight constraints on the 3D spatial and spectral distributions of CRs.

The microwave haze was first detected in the *WMAP* data [2] and later confirmed by *Planck* [3], observed in the $\sim 20 - 40$ GHz band. The haze is spatially coincident with the gamma-ray bubbles, suggesting that they likely share the same origin. Its intensity decays with distance from the GC, consistent with the decaying magnetic field strength within the Galaxy. The microwave haze also has a hard spectrum, which provides key constraints on the formation mechanisms (see § 3). A pair of polarized lobes with similar morphology to the *Fermi* bubbles are also observed at 2.3 GHz by the *S-PASS* survey [10]. The polarized lobes extend to somewhat higher Galactic latitudes ($\sim$ 60 degrees), and their spectrum is steeper than the gamma-ray bubbles, suggesting that they may be generated by a distinct population of CRs. The high polarization fractions within the lobes indicate that the magnetic field within the bubbles are largely coherent.

In the X-ray band, the ROSAT all-sky map has provided a lot of information about the complex thermal gas distribution within the Galactic halo. A pair of X-shaped arc at low Galactic latitudes was detected and proposed to be evidence for a galactic outflow [4]. One of the most prominent features in the X-ray sky is the NPS located in the northern hemisphere. The morphology of the NPS is similar to the Loop I feature seen in the radio sky, and which is believed to be associated with a superbubble in the solar neighborhood [e.g., 11, 12]. However, the NPS also happens to lie near the edge of the *Fermi* bubbles. Therefore, it has been intensely debated whether the NPS is related to a local superbubble, or a GC event of energy injections [e.g., 13–15]. The new *eRosita* data has brought new insights to this dispute, as it revealed a pair of gigantic bubbles in both hemispheres. The existence of the south *eRosita* bubble suggests that at least part of the NPS emission should originate from a GC outburst, supporting a hybrid origin for the NPS [e.g., 16].

In the TeV gamma-ray band, there has also been constraints from the *HAWC* observatory [17]. So far there has been no detection for photon energies above 1 TeV. The obtained upper limits put very stringent constraints on the spectrum of CRs responsible for the gamma-ray emission, disfavoring hadronic models with CR proton (CRp) spectrum extending above 100 TeV. The *IceCube* neutrino observatory has also provided limits on the amount of high-energy neutrinos coming from the region of sky associated with the *Fermi* bubbles. To date, it appears that no significant detections of neutrinos from the Fermi-bubble region have been found, again disfavoring hadronic models with CR spectrum extending to PeV ranges [18, 19]. Other studies have obtained estimates of neutrino fluxes consistent with the level required by the hadronic origin of the *Fermi* bubbles [20]. However, the HAWC upper limits in TeV suggest that these neutrinos are unlikely to be associated with the *Fermi* bubbles.[1]

[1]This neutrino flux could be consistent with the low-latitude ($< 10^\circ$) GeV emission though, which does not have a

There have also been measurements for the thermal, kinematic, and metallicity properties of the Galactic halo using emission/absorption lines in the UV/X-ray bands, which could provide constraints on the potential outflow driven by the GC outburst [see 14, for a more detailed review on this topic]. For instance, [21] extracted X-ray spectra for slightlines passing through the *Fermi* bubbles, and they found metallicity of $Z \sim 0.2\ Z_\odot$ and plasma temperature of $kT \sim 0.3$ keV, higher than typical gas temperature of the halo gas $kT \approx 0.2$ keV. [22] used line ratios between the O VIII and O VII lines of multiple pointings to probe the thermal gas structure within the Galactic halo. Using a simple geometrical model with a volume-filled hot bubble with a shock compressed shell, they obtained constraints on the number density and gas temperature within the shell, $n \approx 10^{-3}$ cm^{-3} and $\log(T) \approx 6.60 - 6.70$. UV absorption line studies of background quasars have also allowed constraints on the velocity structures of the cold gas ($T \sim 10^5$ K) entrained within the galactic outflow [23–26]. Though the interpretation of these observational data and the derived constraints on outflow velocities are highly model dependent (e.g., assumptions about outflow geometry, instantaneous vs. continuous energy injections, timescales for electron-ion equilibrium; see more detailed discussion in [8]), the data offers stringent constraints on the theoretical models proposed to explain the origin of the giant bubbles.

For completeness, one should mention several recent observational evidences for past GC activities. [27] detected an outflow of neutral hydrogen at low Galactic latitudes ($b < 10°$, corresponding to a height of $h \sim 1.5$ kpc) with an outflow velocity of ~ 330 km s^{-1} assuming the outflow opening angle of $\sim 140°$. [28] found bipolar radio bubbles on scales of ~ 15 pc, which are spatially coincident with the GC chimney in X-ray [29]. As the physical scales and required energetics for these phenomena seem quite different from those of the *Fermi/eRosita* bubbles, it remains an open question whether these energetic outbursts have connections with each other.

Figure 1 summarizes all the relevant multi-messenger observational constraints in the vicinity of the *Fermi/eRosita* bubbles. All the spatially resolved, multi-messenger data have offered valuable information for the bubble formation mechanisms and posed stringent constraints on the theoretical models, which will be discussed in § 3.

3. Physical Origin of the Bubbles

Since the discovery of the *Fermi* bubbles in 2010, many theoretical models have been proposed to explain their origin. However, because of the stringent constraints from the ample amount of data available (§ 2), it has been a great challenge for any theoretical model to reproduce the right morphology and spectra of the multi-messenger observational data. In [8] we have reviewed much of the proposed models in detail; in this Conference Proceedings we will highlight the key ideas and more recent developments in terms of the understanding of the bubbles' origin.

To explain the origin of the *Fermi* bubbles and their multi-wavelength counterparts, the following three questions need to be addressed: (1) What is the dominant emission mechanism for the gamma-ray radiation? Is it *leptonic*, in which the gamma-ray emission is produced by IC scattering of the ISRF by CRe, or is it hadronic, where the gamma rays are generated by decay of neutral pions through the hadronic collisions between CRp and ambient protons? (2) What event at the

high-energy cutoff.

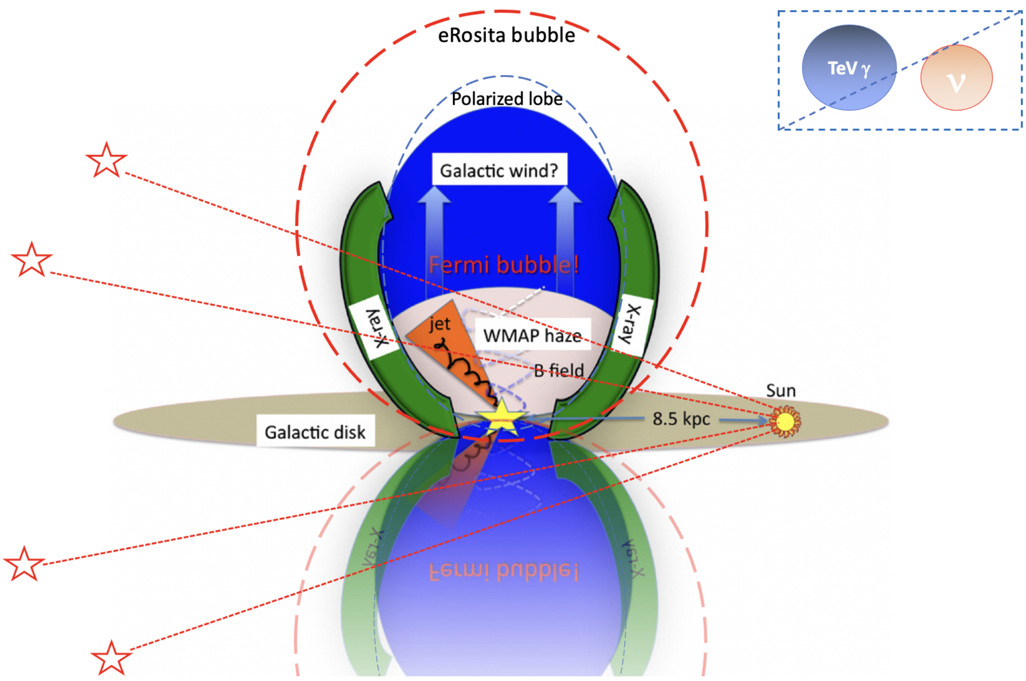

Figure 1: Schematic diagram for all the relevant multi-messenger observational data in the vicinity of the *Fermi/eRosita* bubbles (figure adapted from [1]).

GC triggerred the energy injection that produced the giant bubbles? Are they formed as a result of a nuclear starburst or activity of the GC black hole? (3) Where are the CRs generating the *Fermi* bubbles produced? Are they accelerated close to the GC and transported to large Galactic latitudes, or are they accelerated *in situ* due to shocks or turbulence close to the bubble surface?

Note that because of the hard gamma-ray spectrum of the *Fermi* bubbles, which is well approximated by a power-law spectrum with a spectral index of ~ -2.1 [9], not any of the above combinations of scenarios would work. For instance, if one would like to build a model based on nuclear starburst winds, which would take greater than 10 Myr to reach a height of $\sim$ 10 kpc (with typical wind velocities of hundreds of km s^{-1}), then the gamma-ray emission has to be hadronic, otherwise the high-energy CRe would have cooled due to synchrotron and IC losses before reaching their current location. This scenario is called the "hadronic wind models." If instead one would like to consider a leptonic model, then AGN jets that travel at thousands of km s^{-1} are required to transport the CRs to large distances before they cool – this is the "leptonic jet model." Alternatively, if one would like to bypass all the age constraints from the CRe cooling times altogether, then "in situ acceleration models" need to be invoked, where the CRs are accelerated by shocks or turbulence near the bubble surface. A schematic diagram of the above three categories of models is shown in Figure 2. Note that any of the theoretical models proposed need to fall into one of the three categories.

For the hadronic wind models, it has been shown that they could well reproduce the characteristics of the observed bubbles in the gamma-ray band, either by starburst winds [e.g., 30, 31] or AGN winds [e.g., 32, 33]. However, the synchroton emission produced by the secondary electrons and

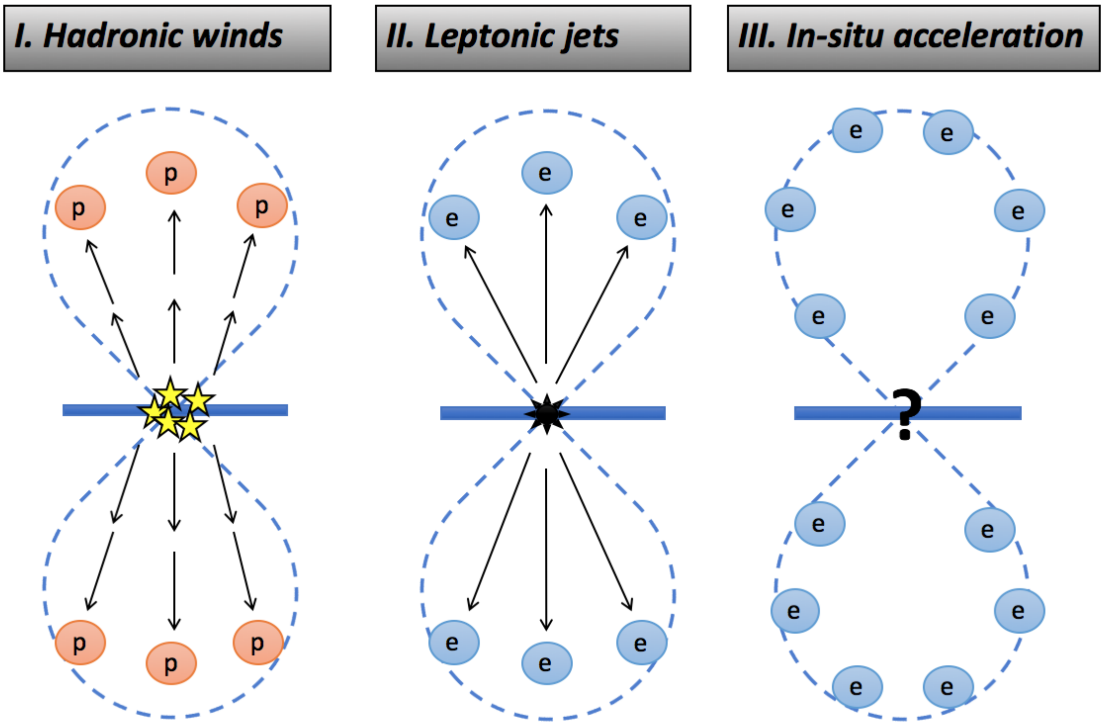

Figure 2: Schematic diagram for the three categories of theoretical models: hadronic wind models, leptonic jet models, and in situ acceleration models. Because of the constraints from the hard gamma-ray spectrum of the *Fermi* bubbles, any theoretical model proposed to explain the bubble formation would need to fall into one of the three scenarios (see text for details).

positrons via the hadronic process falls short in explaining the microwave haze, and the predicted spectrum is too steep compared to the observed one [e.g., 9, 34]. Therefore, purely hadronic models are disfavored, and an additional component of primary electrons needs to be invoked in order to fit the microwave haze spectrum [e.g., 31]. In addition, the HAWC upper limits in TeV as well as the non-detection of neutrinos associated with the *Fermi* bubbles also have ruled out purely hadronic models with CRp spectra extending to PeV energies.

On the other hand, both the leptonic jet model [e.g., 7, 35–39] and the in situ acceleration model [e.g., 40] have shown success in reproducing the gamma-ray and microwave spectra simultaneously with the same population of CRe. In the leptonic jet model, simulations have shown that fast AGN jets could transport the CRe quickly from the GC to large heights within the CRe cooling times of a few Myrs [35, 37]. [39] also showed that the spatially uniform hard gamma-ray spectrum and the high-energy cutoff at $\sim$ 100 GeV [9] could be naturally explained in the leptonic jet scenario. The high-energy cutoff is set by the fast synchrotron and IC cooling of CRe near the GC due to strong magnetic and radiation fields. After the jets leave the central kpc region, the dynamical time of the jets becomes shorter than other cooling timescales, and therefore the CRs are simply advected to large Galactic latitudes within the jet outflow with their spectrum essentially unaltered.

For the in situ acceleration models [e.g., 34, 41–46], the CRs could be accelerated by shocks or turbulence near the bubble surface, so that the hard gamma-ray spectrum and sharp edges of the observed *Fermi* bubbles could be naturally explained. One of the main challenges of the in situ acceleration models is to reproduce the nearly flat intensity profile as observed, because CRs that are shock-accelerated within a thin shell would project into a limb-brightened surface-brightness distribution. To this end, some of the models require efficient escape of CRe [45] or additional component of hadronic CRp [47]. More recently, [40] has demonstrated success in reproducing both the spatially uniform gamma-ray bubble and microwave haze spectra by invoking CRs that are accelerated by turbulence in the downstream of a shock assuming some combinations of CR diffusion coefficients and magnetic field geometry.

The above studies suggest that the leptonic models, either the AGN jet scenario or the stochastic acceleration scenario, seem to be promising proposed theories for explaining the multi-wavelength observable signatures of the giant bubbles/haze. The key question then becomes: which of the leptonic jet model or the in situ acceleration model is correct? Note that, although both models predict similar properties for the nonthermal emission in the gamma-ray and microwave bands, one of the key difference between these two models is the location of the shock front (see Figure 3). In the in situ acceleration models, because the CRs producing the gamma-ray bubbles are generated by shocks or turbulence in the shock downstream, the boundary of the gamma-ray bubbles is expected to coincide with the shock location by construction. On the other hand, in typical AGN jet scenarios, the forward shock is often more extended than the contact discontinuity between the jet materials and the shocked ambient interstellar medium, which corresponds to the surface of the gamma-ray bubbles. Therefore, comparing the location of the shock and boundary of the *Fermi* bubbles would allow us to distinguish the two scenarios.

One could use the X-ray emission to identify the location of the shock driven by the GC outburst, because the shock would compress the gas within the Galactic halo and enhance the local thermal Bremsstrahlung emission in X-ray. The NPS and arc features near the surface of the *Fermi* bubbles seen in the early *ROSAT* all-sky map could indicate the existence of such a shock. However, the sensitivity of *ROSAT* was not yet sufficient to tell whether the shock is coincident with the bubble surface or not. Now with the improved sensitivity of the *eRosita* satellite, one can clearly see the surface of the gigantic *eRosita* bubbles and identify the location of the forward shock. In the overlaid image of the *Fermi* bubbles and the *eRosita* bubbles shown in [6] (their Figure 3), one can clearly see that the boundaries of the gamma-ray and X-ray bubbles are *not* identical to each other. Particularly, the shock front is located further away from the GC than the surface of the gamma-ray bubbles, which is more consistent with the leptonic jet scenario (Figure 3).

Indeed, recent simulations based on the leptonic jet model have demonstrated success in reproducing the morphology and multi-wavelength spectra of the observed *Fermi* bubbles, *eRosita* bubbles, and the microwave haze [7]. Using 3D magnetohydroydnamic (MHD) simulations including self-consistent modeling of the evolution of the CR spectra, it was found that these gigantic structures in the Milky Way Galaxy could be simultaneously explained by a single jet event from the central supermassive black hole Sgr A* ~ 2.6 Myrs ago. The separation between the forward shock and the contact discontinuity allows tighter constraints to be put on the duration of the jet injections compared to previous results using morphology of the gamma-ray bubbles alone [37], yielding an estimate of ~ 0.1 Myr as the duration of the black hole accretion event. During its active phase, the central black hole is estimated to be accreting at a rate $\sim 1 - 10\%$ of the Eddington rate, which corresponds to a total $\sim 10^{3-4}\ M_\odot$ of materials being accreted onto the black hole. Interestingly,

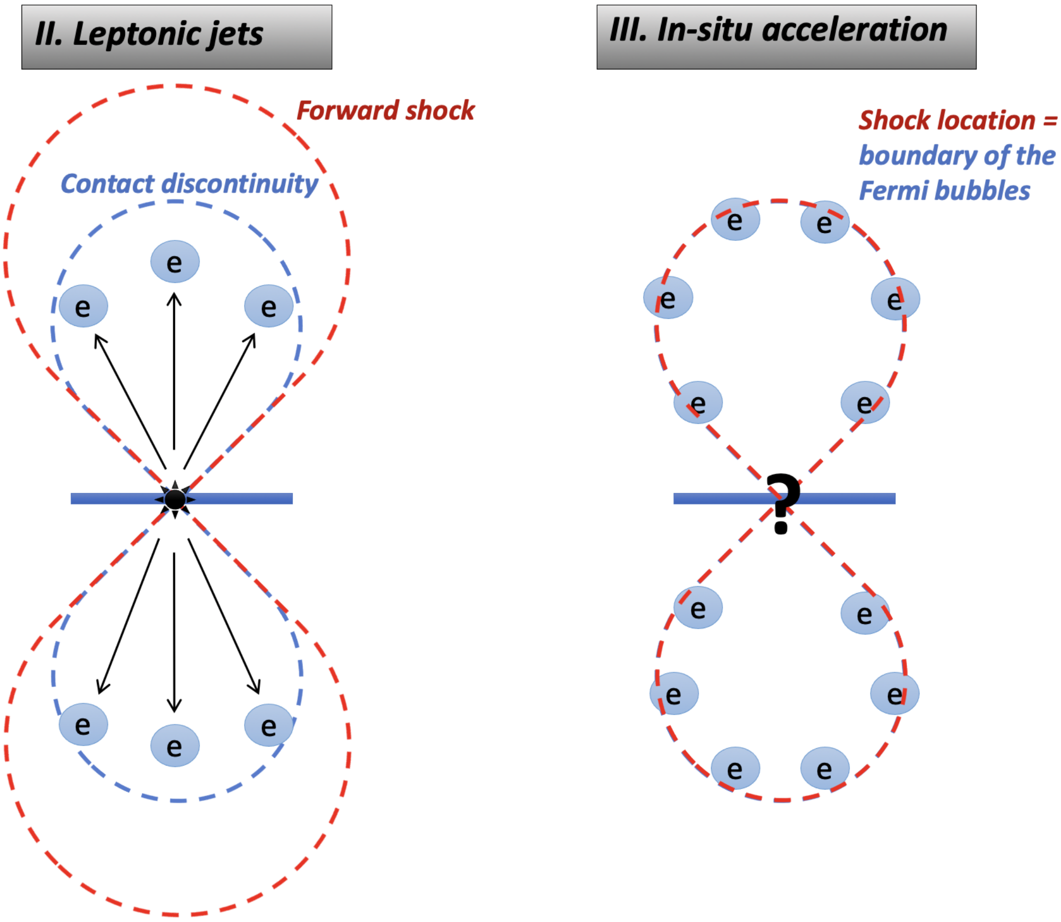

Figure 3: Schematic diagram comparing the expected shock location and surface of the *Fermi* bubbles in the leptonic jet scenario (left) versus the in situ acceleration models.

the timescales and energetics estimated for the leptonic jet model are consistent with independent constraints from elevated ionization signatures in the Magellanic Stream [48–50]. Specifically, it was found that there are enhanced ionization in H_α, C IV, and Si IV along the south Galactic pole, which can be naturally explained by a Seyfert-flare model proposed by [48, 49]. The similarity of the inferred timescales and activity level of the Sgr A* from these independent constraints suggests that the GC black hole indeed could have gone through an active period in the past few Myrs.

4. Open Questions and Future Prospects

The new observational constraints from *eRosita* have highlighted the power of combining multi-messenger data to gain insights into the formation scenarios of these fascinating structures in our Milky Way Galaxy. Despite the recent progress, there remain many opening questions to be addressed in the future. We discuss some of the open questions and future prospects in the following.

- **Could the leptonic jet model fit the thermal, kinematic, and metallicity constraints of the Galacitc halos?** While the leptonic jet model is successful in reproducing the observed nonthermal signatures and integrated X-ray emission, it remains to be shown whether it is consistent with X-ray/UV emission/absorption line studies of the Galactic halo.[2] As mentioned in § 2, the interpretation of the observational data can be affected by several simplified assumptions in the modeling, and hence it is critical to verify the model using a forward-modeling approach and make detailed comparisons between the model and the observational data.

- **Are the jet directions required to be perpendicular to the Galactic plane?** Motivated by the symmetry of the observed *Fermi/eRosita* bubbles, previous works that considered the leptonic jet models [e.g., 7, 35, 37] have considered energy injections perpendicular to the Galactic plane. However, in general the direction of black hole jets does not need to align with the rotational axis of the host galaxy. Also, recent constraints from the shadow of Sgr A* suggest that the black hole spin *at the present day* could have a low inclination angle [51].[3] Therefore, more studies are required to explore possibilities in which the jets are tilted with respect to the Galactic plane, and see whether they could still produce symmetric bubbles after the jets interact with the dense, clumpy interstellar medium within the Galactic disk [e.g., 53].

- **Could we detect Fermi-bubble analogues in nearby galaxies?** In order to make connections between the GC outburst that generated the *Fermi* bubbles to activities in other galaxies in general, one useful piece of information is how frequently do similar events occur, and one way to tell is by searching for Fermi-bubble analogues in nearby Milky-Way-like galaxies. Recently, [54] and [55] have investigated the evolution of the multi-wavelength spectra of galaxies bubbles similar to the *Fermi* bubbles in both the leptonic and hadronic scenarios. It was found that, for the leptonic scenario, the CRe cool very quickly due to synchrotron and IC cooling. Therefore, their TeV emission decays very quickly, and only a few would be observable even with the sensitivity of Cherenkov Telescope Array (CTA). On the other hand, the radio emission does not drop significantly over time, and thus a few dozens may be observable with the sensitivity similar to Square Kilometer Array (SKA).

- **How do AGN jets affect the evolution of Milky-Way like galaxies?** In the current understanding of jet-mode or radio-mode AGN feedback, typically the discussion is focused on its influence on suppressing cooling flows in giant elliptical galaxies and clusters of galaxies. However, if the *Fermi/eRosita* bubbles are truly generated by AGN jets, it would be interesting to ask whether such jets could also provide feedback and suppress subsequent star formation activities in lower-mass, star forming galaxies like the Milky Way. Simulations [e.g., 56] have demonstrated that star formation rates in galaxies could be substantially reduced by AGN jet-driven turbulence, depending on the jet power and inclination. It remains an open question

[2] Note that there remain some parameter degeneracies in the leptonic jet model which would make different predictions for the gas temperature inside the *Fermi* bubbles [7]. Therefore we plan to investigate this issue in future work.

[3] Of course, the black hole spin axis at the present day does not need to be the same as a few Myrs ago. In addition, there could be efficient black hole spin-galaxy disk alignment processes in low-mass galaxies [e.g., 52].

how to link the powerful outburst in the Milky Way to the overall picture of SMBH-galaxy coevolution.

References

[1] Su, M.; Slatyer, T.R.; Finkbeiner, D.P. Giant Gamma-ray Bubbles from Fermi-LAT: Active Galactic Nucleus Activity or Bipolar Galactic Wind? **2010**, *724*, 1044–1082, [arXiv:astro-ph.HE/1005.5480].

[2] Finkbeiner, D.P. Microwave Interstellar Medium Emission Observed by the Wilkinson Microwave Anisotropy Probe. **2004**, *614*, 186–193, [arXiv:astro-ph/0311547].

[3] Planck Collaboration. Planck intermediate results. IX. Detection of the Galactic haze with Planck. **2013**, *554*, A139, [arXiv:astro-ph.GA/1208.5483].

[4] Bland-Hawthorn, J.; Cohen, M. The Large-Scale Bipolar Wind in the Galactic Center. **2003**, *582*, 246–256, [astro-ph/0208553].

[5] Snowden, S.L.; others. ROSAT Survey Diffuse X-Ray Background Maps. II. **1997**, *485*, 125.

[6] Predehl, P.; Sunyaev, R.A.; Becker, W.; Brunner, H.; Burenin, R.; Bykov, A.; Cherepashchuk, A.; Chugai, N.; Churazov, E.; Doroshenko, V.; Eismont, N.; Freyberg, M.; Gilfanov, M.; Haberl, F.; Khabibullin, I.; Krivonos, R.; Maitra, C.; Medvedev, P.; Merloni, A.; Nandra, K.; Nazarov, V.; Pavlinsky, M.; Ponti, G.; Sanders, J.S.; Sasaki, M.; Sazonov, S.; Strong, A.W.; Wilms, J. Detection of large-scale X-ray bubbles in the Milky Way halo. **2020**, *588*, 227–231, [arXiv:astro-ph.GA/2012.05840].

[7] Yang, H.Y.K.; Ruszkowski, M.; Zweibel, E.G. Fermi and eROSITA bubbles as relics of the past activity of the Galaxy's central black hole. *Nature Astronomy* **2022**, *6*, 584–591, [arXiv:astro-ph.HE/2203.02526].

[8] Yang, H.Y.; Ruszkowski, M.; Zweibel, E. Unveiling the Origin of the Fermi Bubbles. *Galaxies* **2018**, *6*, 29, [arXiv:astro-ph.HE/1802.03890].

[9] Ackermann, M.; Albert, A.; Atwood, W.B.; others. The Spectrum and Morphology of the Fermi Bubbles. **2014**, *793*, 64, [arXiv:astro-ph.HE/1407.7905].

[10] Carretti, E.; others. Giant magnetized outflows from the centre of the Milky Way. **2013**, *493*, 66–69, [arXiv:astro-ph.GA/1301.0512].

[11] Berkhuijsen, E.M.; Haslam, C.G.T.; Salter, C.J. Are the galactic loops supernova remnants? **1971**, *14*, 252.

[12] Das, K.K.; Zucker, C.; Speagle, J.S.; Goodman, A.; Green, G.M.; Alves, J. Constraining the distance to the North Polar Spur with Gaia DR2. **2020**, *498*, 5863–5872, [arXiv:astro-ph.GA/2009.01320].

[13] Sofue, Y. Bipolar Hypershell Galactic Center Starburst Model: Further Evidence from ROSAT Data and New Radio and X-Ray Simulations. **2000**, *540*, 224–235, [arXiv:astro-ph/astro-ph/9912528].

[14] Kataoka, J.; Sofue, Y.; Inoue, Y.; Akita, M.; Nakashima, S.; Totani, T. X-Ray and Gamma-Ray Observations of the Fermi Bubbles and NPS/Loop I Structures. *Galaxies* **2018**, *6*, 27.

[15] LaRocca, D.M.; Kaaret, P.; Kuntz, K.D.; Hodges-Kluck, E.; Zajczyk, A.; Bluem, J.; Ringuette, R.; Jahoda, K.M. An Analysis of the North Polar Spur Using HaloSat. *The Astrophysical Journal* **2020**, *904*, 54.

[16] Panopoulou, G.V.; Dickinson, C.; Readhead, A.C.S.; Pearson, T.J.; Peel, M.W. Revisiting the Distance to Radio Loops I and IV Using Gaia and Radio/Optical Polarization Data. **2021**, *922*, 210, [arXiv:astro-ph.GA/2106.14267].

[17] Abeysekara, A.U.; Albert, A.; Alfaro, R.; Alvarez, C.; Álvarez, J.D.; Arceo, R.; Arteaga-Velázquez, J.C.; Ayala Solares, H.A.; Barber, A.S.; Bautista-Elivar, N.; et al.. Search for Very High-energy Gamma Rays from the Northern Fermi Bubble Region with HAWC. **2017**, *842*, 85.

[18] Fang, K.; Su, M.; Linden, T.; Murase, K. IceCube and HAWC constraints on very-high-energy emission from the Fermi bubbles. **2017**, *96*, 123007, [arXiv:astro-ph.HE/1704.03869].

[19] Sherf, N.; Keshet, U.; Gurwich, I. IceCube Constraints on the Fermi Bubbles. **2017**, *847*, 95, [arXiv:astro-ph.HE/1705.06665].

[20] Lunardini, C.; Razzaque, S.; Yang, L. Multimessenger study of the Fermi bubbles: Very high energy gamma rays and neutrinos. **2015**, *92*, 021301, [arXiv:astro-ph.HE/1504.07033].

[21] Kataoka, J.; Tahara, M.; Totani, T.; Sofue, Y.; Inoue, Y.; Nakashima, S.; Cheung, C.C. Global Structure of Isothermal Diffuse X-Ray Emission along the Fermi Bubbles. **2015**, *807*, 77, [arXiv:astro-ph.HE/1505.05936].

[22] Miller, M.J.; Bregman, J.N. The Interaction of the Fermi Bubbles with the Milky Ways Hot Gas Halo. **2016**, *829*, 9, [1607.04906].

[23] Fox, A.J.; Bordoloi, R.; Savage, B.D.; Lockman, F.J.; Jenkins, E.B.; Wakker, B.P.; Bland-Hawthorn, J.; Hernandez, S.; Kim, T.S.; Benjamin, R.A.; Bowen, D.V.; Tumlinson, J. Probing the Fermi Bubbles in Ultraviolet Absorption: A Spectroscopic Signature of the Milky Way's Biconical Nuclear Outflow. **2015**, *799*, L7, [1412.1480].

[24] Bordoloi, R.; Fox, A.J.; Lockman, F.J.; Wakker, B.P.; Jenkins, E.B.; Savage, B.D.; Hernandez, S.; Tumlinson, J.; Bland-Hawthorn, J.; Kim, T.S. Mapping the Nuclear Outflow of the Milky Way: Studying the Kinematics and Spatial Extent of the Northern Fermi Bubble. **2017**, *834*, 191, [1612.01578].

[25] Karim, T.; Fox, A.J.; Jenkins, E.B.; Bordoloi, R.; Wakker, B.P.; Savage, B.D.; Lockman, F.J.; Crawford, S.M.; Jorgenson, R.A.; Bland-Hawthorn, J. Probing the Southern Fermi Bubble in Ultraviolet Absorption Using Distant AGNs. **2018**, *860*, 98, [arXiv:astro-ph.GA/1804.10617].

[26] Ashley, T.; Fox, A.J.; Jenkins, E.B.; Wakker, B.P.; Bordoloi, R.; Lockman, F.J.; Savage, B.D.; Karim, T. Mapping Outflowing Gas in the Fermi Bubbles: A UV Absorption Survey of the Galactic Nuclear Wind. **2020**, *898*, 128.

[27] Teodoro, E.M.D.; McClure-Griffiths, N.M.; Lockman, F.J.; Denbo, S.R.; Endsley, R.; Ford, H.A.; Harrington, K. Blowing in the Milky Way Wind: Neutral Hydrogen Clouds Tracing the Galactic Nuclear Outflow. *The Astrophysical Journal* **2018**, *855*, 33.

[28] Heywood, I.; Camilo, F.; Cotton, W.D.; Yusef-Zadeh, F.; Abbott, T.D.; Adam, R.M.; Aldera, M.A.; Bauermeister, E.F.; Booth, R.S.; Botha, A.G.; et al.. Inflation of 430-parsec bipolar radio bubbles in the Galactic Centre by an energetic event. *Nature* **2019**, *573*, 235–237.

[29] Ponti, G.; Hofmann, F.; Churazov, E.; Morris, M.R.; Haberl, F.; Nandra, K.; Terrier, R.; Clavel, M.; Goldwurm, A. An X-ray chimney extending hundreds of parsecs above and below the Galactic Centre. *Nature* **2019**, *567*, 347–350.

[30] Crocker, R.M.; Aharonian, F. Fermi Bubbles: Giant, Multibillion-Year-Old Reservoirs of Galactic Center Cosmic Rays. *Physical Review Letters* **2011**, *106*, 101102, [arXiv:astro-ph.GA/1008.2658].

[31] Crocker, R.M.; Bicknell, G.V.; Taylor, A.M.; Carretti, E. A Unified Model of the Fermi Bubbles, Microwave Haze, and Polarized Radio Lobes: Reverse Shocks in the Galactic Centers Giant Outflows. **2015**, *808*, 107, [arXiv:astro-ph.HE/1412.7510].

[32] Mou, G.; Yuan, F.; Bu, D.; Sun, M.; Su, M. Fermi Bubbles Inflated by Winds Launched from the Hot Accretion Flow in Sgr A*. **2014**, *790*, 109, [arXiv:astro-ph.HE/1403.2129].

[33] Mou, G.; Yuan, F.; Gan, Z.; Sun, M. The Accretion Wind Model of Fermi Bubbles. II. Radiation. **2015**, *811*, 37, [arXiv:astro-ph.HE/1505.00892].

[34] Cheng, K.S.; Chernyshov, D.O.; Dogiel, V.A.; Ko, C.M. Multi-wavelength Emission from the Fermi Bubble. II. Secondary Electrons and the Hadronic Model of the Bubble. **2015**, *799*, 112, [1411.6395].

[35] Guo, F.; Mathews, W.G. The Fermi Bubbles. I. Possible Evidence for Recent AGN Jet Activity in the Galaxy. **2012**, *756*, 181, [arXiv:astro-ph.HE/1103.0055].

[36] Guo, F.; Mathews, W.G.; Dobler, G.; Oh, S.P. The Fermi Bubbles. II. The Potential Roles of Viscosity and Cosmic-Ray Diffusion in Jet Models. **2012**, *756*, 182, [arXiv:astro-ph.HE/1110.0834].

PoS(ECRS)023

[37] Yang, H.Y.K.; Ruszkowski, M.; Ricker, P.M.; Zweibel, E.; Lee, D. The Fermi Bubbles: Supersonic Active Galactic Nucleus Jets with Anisotropic Cosmic-Ray Diffusion. **2012**, *761*, 185, [arXiv:astro-ph.GA/1207.4185].

[38] Yang, H.Y.K.; Ruszkowski, M.; Zweibel, E. The Fermi bubbles: gamma-ray, microwave and polarization signatures of leptonic AGN jets. **2013**, *436*, 2734–2746, [arXiv:astro-ph.GA/1307.3551].

[39] Yang, H.Y.K.; Ruszkowski, M. The Spatially Uniform Spectrum of the Fermi Bubbles: The Leptonic Active Galactic Nucleus Jet Scenario. **2017**, *850*, 2.

[40] Mertsch, P.; Petrosian, V. Fermi bubbles from stochastic acceleration of electrons in a Galactic outflow. *Astronomy Astrophysics* **2019**, *622*, A203.

[41] Cheng, K.S.; Chernyshov, D.O.; Dogiel, V.A.; Ko, C.M.; Ip, W.H. Origin of the Fermi Bubble. **2011**, *731*, L17, [arXiv:astro-ph.HE/1103.1002].

[42] Mertsch, P.; Sarkar, S. Fermi Gamma-Ray "Bubbles" from Stochastic Acceleration of Electrons. *Physical Review Letters* **2011**, *107*, 091101, [arXiv:astro-ph.HE/1104.3585].

[43] Lacki, B.C. The Fermi bubbles as starburst wind termination shocks. **2014**, *444*, L39–L43, [arXiv:astro-ph.HE/1304.6137].

[44] Fujita, Y.; Ohira, Y.; Yamazaki, R. A Hadronic-leptonic Model for the Fermi Bubbles: Cosmic-Rays in the Galactic Halo and Radio Emission. **2014**, *789*, 67, [arXiv:astro-ph.HE/1405.5214].

[45] Sasaki, K.; Asano, K.; Terasawa, T. Time-dependent Stochastic Acceleration Model for Fermi Bubbles. **2015**, *814*, 93, [arXiv:astro-ph.HE/1510.02869].

[46] Sarkar, K.C.; Nath, B.B.; Sharma, P. Multiwavelength features of Fermi bubbles as signatures of a Galactic wind. **2015**, *453*, 3827–3838, [1505.03634].

[47] Fujita, Y.; Ohira, Y.; Yamazaki, R. The Fermi Bubbles as a Scaled-up Version of Supernova Remnants. **2013**, *775*, L20, [arXiv:astro-ph.HE/1308.5228].

[48] Bland-Hawthorn, J.; Maloney, P.R.; Sutherland, R.S.; Madsen, G.J. Fossil Imprint of a Powerful Flare at the Galactic Center along the Magellanic Stream. **2013**, *778*, 58, [1309.5455].

[49] Bland-Hawthorn, J.; Maloney, P.R.; Sutherland, R.; Groves, B.; Guglielmo, M.; Li, W.; Curzons, A.; Cecil, G.; Fox, A.J. The Large-scale Ionization Cones in the Galaxy. **2019**, *886*, 45, [arXiv:astro-ph.GA/1910.02225].

[50] Fox, A.J.; Frazer, E.M.; Bland-Hawthorn, J.; Wakker, B.P.; Barger, K.A.; Richter, P. Kinematics of the Magellanic Stream and Implications for Its Ionization. *The Astrophysical Journal* **2020**, *897*, 23.

[51] Event Horizon Telescope Collaboration. First Sagittarius A* Event Horizon Telescope Results. I. The Shadow of the Supermassive Black Hole in the Center of the Milky Way. *The Astrophysical Journal Letters* **2022**, *930*, L12.

[52] Fiacconi, D.; Sijacki, D.; Pringle, J.E. Galactic nuclei evolution with spinning black holes: method and implementation. **2018**, *477*, 3807–3835.

[53] Sarkar, K.C.; Mondal, S.; Sharma, P.; Piran, T. Misaligned jets from Sgr A* and the origin of Fermi/eROSITA bubbles. *arXiv e-prints* **2022**, p. arXiv:2211.12967, [arXiv:astro-ph.HE/2211.12967].

[54] Owen, E.R.; Yang, H.Y.K. Emission from hadronic and leptonic processes in galactic jet-driven bubbles. **2022**, *516*, 1539–1556, [arXiv:astro-ph.HE/2111.01402].

[55] Owen, E.R.; Yang, H.Y.K. Emission from hadronic and leptonic processes in galactic jet-driven bubbles. **2022**, *516*, 1539–1556, [arXiv:astro-ph.HE/2111.01402].

[56] Mukherjee, D.; Bicknell, G.V.; Wagner, A.Y.; Sutherland, R.S.; Silk, J. Relativistic jet feedback - III. Feedback on gas discs. **2018**, *479*, 5544–5566, [arXiv:astro-ph.HE/1803.08305].